Broadband near-zero index metamaterials

Konstantinidis, K; Feresidis, A P

DOI:
10.1088/2040-8978/17/10/105104

Document Version
Peer reviewed version

Citation for published version (Harvard):
Konstantinidis, K & Feresidis, AP 2015, 'Broadband near-zero index metamaterials', *Journal of Optics*, vol. 17, no. 10, pp. 105104. https://doi.org/10.1088/2040-8978/17/10/105104

Broadband near-zero index metamaterials

K. Konstantinidis, A. P. Feresidis
School of Electronic, Electrical and Systems Engineering, University of Birmingham,
Edgbaston, Birmingham B15 2TT, UK

Abstract

We present a new type of Near Zero Index (NZI) and Epsilon-Near-Zero (ENZ) metametarial with broad bandwidth characteristics. We propose an optimal geometry to manipulate the properties of the composite material and realize a metallic-dielectric NZI effective material operating at microwave frequencies with a broadband near zero response. The effective material is composed by multiple layers of dissimilar metasurfaces of subwavelength dimensions. We demonstrate the broadband NZI metamaterial properties and study its anisotropy by realising a radiating structure exhibiting broadband directive emission. An experimental demonstration validates the concept for an antenna in the microwave domain.

1. Introduction

Over the past years metamaterials have been the subject of extensive study due to their extraordinary properties. They offer great flexibility for manipulating their electromagnetic and optical properties such as their effective refractive index. Negative-index metamaterials have been realised and experimentally demonstrated [4, 5]. More recently, numerous reports have appeared for metamaterials with near-zero refractive index (NZI) [1] and epsilon-near-zero (ENZ) [2, 3] for visible and infrared wavelengths. Electromagnetic waves inside such materials experience no spatial phase change and extremely large phase velocity. These properties pave the way for a number of applications such as cloaking [6-8], super-reflection [9], tunnelling [10-12] and funnelling [13].

Metasurfaces [14, 15] are a 2D implementation of metamaterial structures, typically created by arrays of sub-wavelength scatterers. NZI metasurfaces have been employed in conjunction with low directive emission sources to achieve directivity enhancement [16-18]. In these studies, multiple layers of metasurfaces have been utilized resulting in a bulky profile. The design of sub-wavelength profile metasurfaces for directive emission has been also investigated [19-21] exploiting the unique property of Artificial Magnetic Conductor (AMC) surfaces to reflect electromagnetic waves with zero phase shift at a specific frequency. This type of metasurfaces where introduced in [22] and are formed by a periodic arrangement of metallic patches on a grounded dielectric substrate. However, all the aforementioned antenna structures exhibit very narrow bandwidth due to the respectively narrowband NZI response.

In this Letter we present an implementation of broadband NZI metamaterial and we demonstrate its properties experimentally by using it to produce broadband directive emission by a single low directivity source. In particular, we propose multiple layers of closely spaced metasurfaces designed to manipulate the constitutive parameters of the effective metamaterial. The retrieval parameters are extracted using the reflection and transmission characteristics of the metamaterial [23-25], demonstrating the broadband NZI effect which is produced by creating a negative group delay in the reflection mode of the structure. The parameters have been extracted considering both isotropic and anisotropic homogeneous material. Although more rigorous techniques for the extraction of metamaterial constitutive parameter can be employed based on averaging fields [26], we focus here

on the standard retrieval technique. In addition, introducing a low directive radiating source between a conducting plane and the proposed composite metasurfaces, a broadband directional antenna is generated. A validation of the concept is also presented by comparing the radiation patterns of the antenna formed using the proposed metasurfaces, with the patterns calculated for a homogeneous material with the extracted effective retrieval parameters.

2. Design of broadband near-zero index metasurfaces

In Fig. 1, the structure of the created antenna is depicted, with the metamaterial studied in this Letter placed above a conducting plane and a radiating source as explained earlier. The metamaterial consist of a combination of two double-layer arrays of scatterers with dissimilar subwavelength dimensions printed on either sides of a dielectric sheet and separated by an air cavity. Each composite double-layer structure comprises a capacitive and an inductive metasurface resulting in a total of four metasurfaces (Fig. 1). The thickness of each of the two dielectric sheets is 1.5mm and the dielectric permittivity is ε_r=2.2. The capacitive and inductive surfaces are formed by square conducting elements and square apertures on a conducting sheet respectively, shifted with respect to each other.

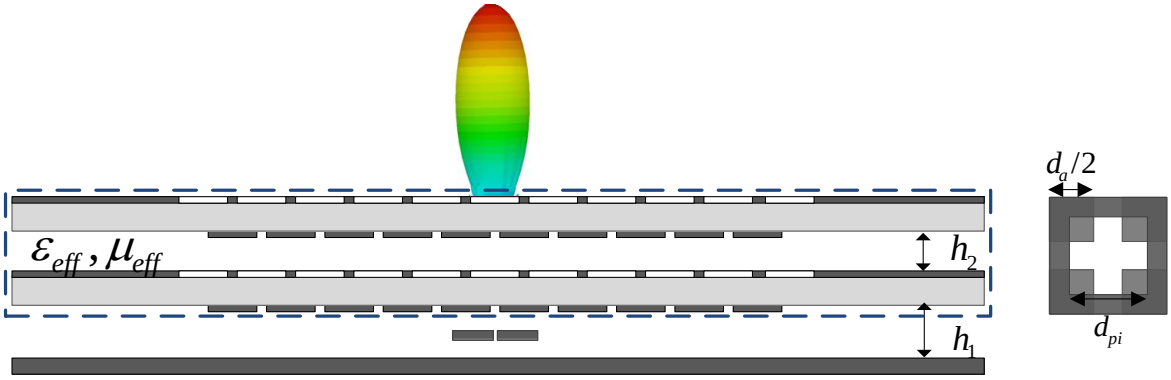

FIG. 1 Schematic diagram of the antenna generated utilizing the two pairs of composite metasurfaces with subwavelength separation h_2=4.8mm placed at distance h_1=5.6mm (~λ/4 at 15GHz) above a conducting plane and a dipole source. Each metasurface has a lateral size of around 4 λ. The unit cell of each pair of metasurfaces is depicted at the right with period p=5.5mm. For both capacitive arrays the dimension of the square scatterers is d_a=4mm. The apertures for the inductive arrays are d_{p1}=3.4mm and d_{p2}=3.7mm for the first and the second metasurface pairs respectively. The effective homogeneous metamaterial is also illustrated with the blue dashed line, with effective parameters ε_{eff} and μ_{eff}. This antenna structure will lead to broadband directive emission with radiation beams at broadside as the one depicted in this figure.

In order to evaluate the constitutive parameters of the designed metamaterial, we consider infinite size metasurfaces with the dimensions and separation described above. The unit cell of the composed metamaterial structure is modelled using an electromagnetic simulation software [27] after applying periodic boundary conditions and the scattering parameters (S-parameters) are extracted for normal plane wave incidence as shown in Fig. 2(a). The reflection coefficient (R) and the transmission coefficient (T) show strong modulation with frequency within the range 13-14GHz. Subsequently, using the analytical expressions described in [23, 24], considering an isotropic metamaterial, the refractive index as well as the electric permittivity ε and magnetic permeability μ are calculated. The real part of the permittivity undergoes an inverse spectral variation from 13.2GHz to 14.2GHz. The resulting fluctuation in the real permittivity values produces a second zero crossing with the values between the two zeros being very small. After this point epsilon continues increasing. A similar fluctuating response is observed in the magnetic permeability which is approaching zero at 13.5GHz. The combination of epsilon and mu values results in the refractive index shown in Fig. 2(b). The real part of n has small values within the range of 0.5 and 0.8 in the frequency range of interest, i.e. the

range where the NZI effect is obtained. It should be pointed out that this effect has been attained by engineering the properties of each metasurface and controlling their individual dimensions so that their specific combination will provide the presented broadband NZI response.

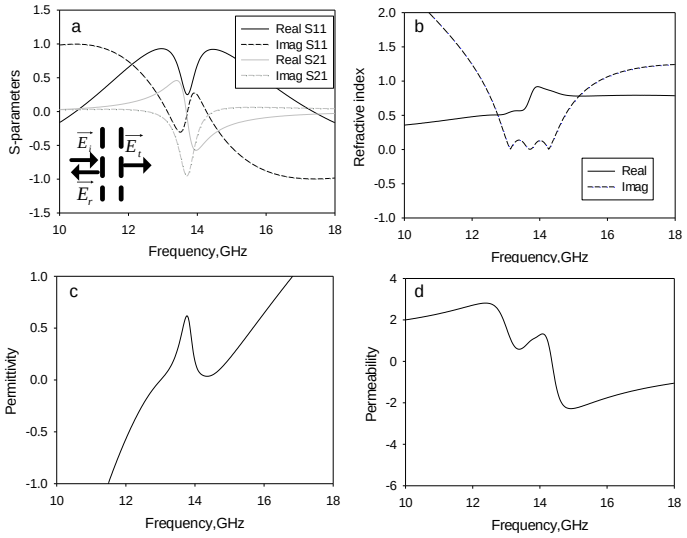

FIG. 2 (a) Reflection (R) and transmission (T) coefficients under normal incidence for two metasurfaces of dissimilar reflectivities, optimized to achieve a negative group delay response in the reflection mode. (b)Refractive index n for the proposed metamaterial structure as calculated with the retrieval method considering isotropic effective medium. (c) Effective electric permittivity and (d) Effective magnetic permeability.

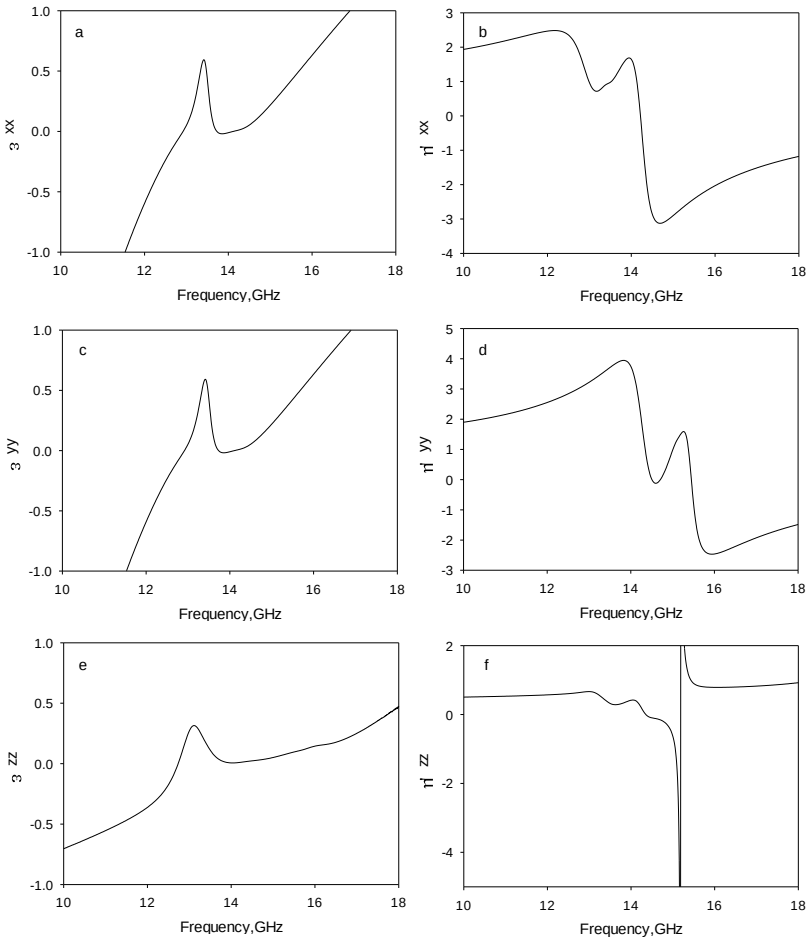

FIG. 3 Effective electric permittivity (a) for the x direction, (c) for the y direction and (e) for the z direction of the optimized composite metasurfaces. The respective effective magnetic permeabilities are plotted in subfigures (b), (d) and (f). The above parameters have been estimated for anisotropic effective medium utilizing the modified retrieval parameter extraction method cited in [25].

The evaluation of the parameters presented above has been carried out under the hypothesis of an isotropic effective medium. A more accurate characterization of the proposed metasurfaces is carried out that takes into account the anisotropy of the proposed metamaterial in the x, y, z axes. In order to gauge the constitutive parameters for anisotropic materials, the modelled scattering parameters for two different angles of incidence were used as explained in [25], to obtain information for all three components of the electric and magnetic fields. Again, we consider infinite size metasurfaces and the scattering parameters are extracted for a set of incident angles for both transverse-electric (TE) and transverse-magnetic (TM) incident waves. The modified analytical expressions proposed in [25] are then used, and the electric permittivity ε and magnetic permeability μ tensors are computed and shown in Fig. 3. It can be observed, that the obtained response for the three orientations exhibit qualitative similarities to the one of the isotropic case. In particular, in the x and y directions the ε and μ are very similar (Fig. 3(a), (c) and (b), (d)), as expected due to the symmetry of the structure in these directions. Once again, the real part of the permittivity undergoes an inverse variation around 13.8GHz, crossing zero at about 13GHz and 14.2GHz. This effect is observed for all three dimensions. However, for the z-axis, which is the one we are mostly interested in as it is the main direction of propagation, ε_{zz} assumes values closer to zero and for a slightly broader frequency range compared to x and y. Particularly, ε_{zz} is below 0.4 within the frequency range of interest, while for ε_{xx} and ε_{yy} the local maximum of the real part is 0.6. Additionally, the magnetic permeability experiences a fluctuation at the frequencies where ε shows the inverse variation with frequency. Specifically, for μ_{zz} the values are also close to zero (less than 0.5), while a discontinuity occurs above 15GHz which is outside our range of interest.

The NZI effect could be extended to cover a broader bandwidth by altering the dimensions of the metasurfaces to adequately manipulate their total reflectivity. A reduced total reflectivity will result to a higher peak value of ε, leading to a more broadband behavior. On the contrary, an increase in the total reflectivity of the metamaterial structure will result in a lower peak value and narrower frequency range of NZI. This property of the proposed metasurfaces can be further extended, keeping the same low value of ε, by adding extra layers of properly designed metasurfaces. However for the specific example, constrained by two pairs of composite metasurfaces, the optimum balance between a close to zero permittivity and bandwidth has been reached.

3. Application for high-gain antenna

As an application of the proposed metasurfaces, which exploits the NZI property, we incorporate them with a low directivity dipole source in order to generate a highly directive antenna. This is one of the several potential applications of NZI materials. The structure is shown in Fig. 1 and it consists of the designed metasurfaces placed above a conducting plane and a low directive radiating source. Due to the broadband NZI response, a broad frequency range of high directive emission is obtained as demonstrated by the radiation patterns shown in Fig. 4 for 13.4GHz and 14GHz. The results were obtained by simuating the whole structure in an electromagnetic simulation software [26]. The value of the maximum directivity obtained by the modeled structure is 18.2dB. Furthermore, a homogeneous anisotropic material is modeled using the extracted constitutive parameter values plotted in Fig. 3. This effective material has replaced the multi-layer metasurfaces, shown in Fig. 1 with the blue dashed line, and the radiation patterns for this case have also been extracted. A

comparison between the patterns produced by the proposed metasurfaces and the anisotropic effective medium is illustrated in Fig. 4. The same study has been carried out for an isotropic material. However, taking into account the anisotropy of the structure, better agreement has been obtained. Moreover, the electric field distributions for the two representative frequencies are illustrated in Fig. 5 for both H- and E-planes. It can be seen that in all cases, the electric field emanating from the dipole source excites the NZI medium, whether it is the anisotropic effective medium or the composite proposed metamaterial, and creates a relatively smooth near-uniform distribution which in turn produces the highly directive beams in both planes. Of course, some discrepancies between the field distributions of the effective medium and the composite metamaterial are observed and expected due to the periodic non-homogeneous nature of the metamaterial structures.

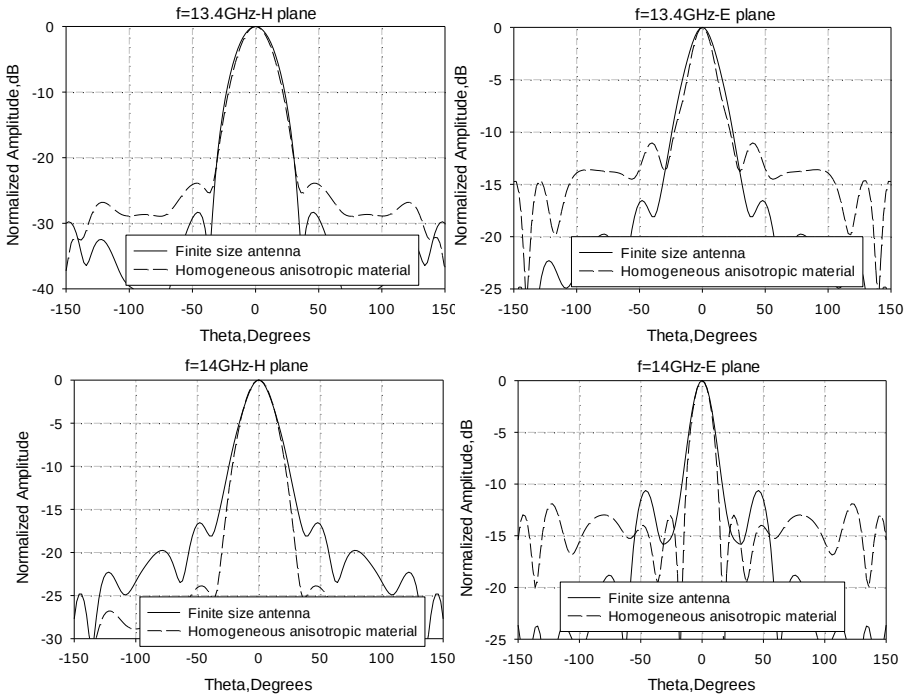

FIG. 4 Radiation patterns comparison between the proposed structure and homogeneous anisotropic material for H-plane and E-plane at 13.4GHz and 14GHz.

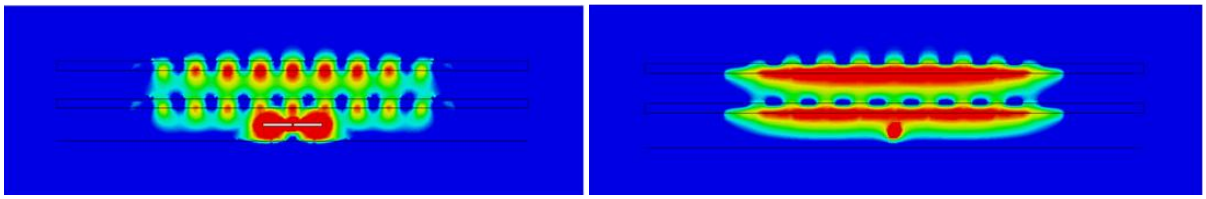

(a)

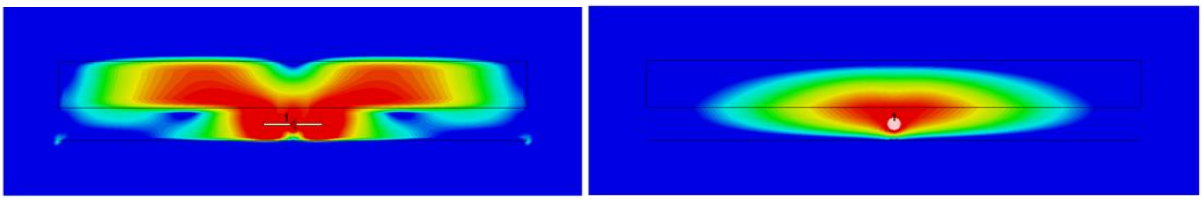

(b)

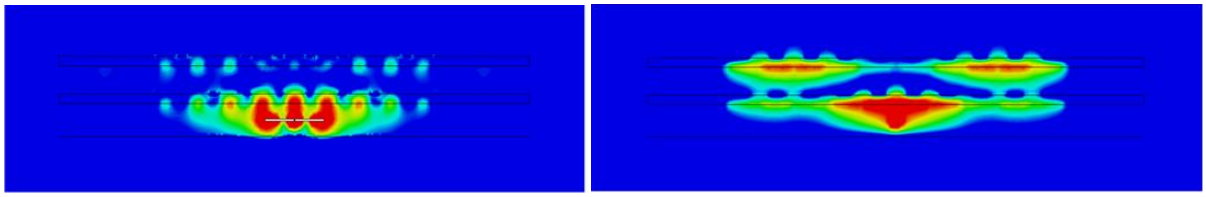

(c) would it look a bit better if you slightly decreased the minimum value here..?

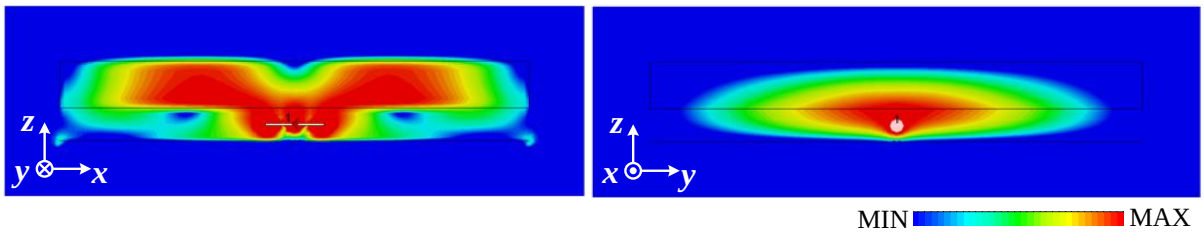

(d)

FIG. 5 Electric field distribution of the proposed antenna structure at (a) 13.4GHz and (c)14GHz and the homogeneous anisotropic material at (b)13.4GHz and (d)14GHz. H-plane and E-plane is shown at the left and right respectively.

4. Fabricated prototype and measurements

Finally an experimental demonstration of the effect produced by employing the designed subwavelength metasurfaces was carried out. A practical feeding source for the antenna was implemented, comprising two rectangular apertures at the conducting plane, fed by a microstrip line. The dimensions were chosen to obtain an impedance matching between the source and the metasurfaces within the frequency range of interest. The complete antenna structure formed by the multi-layer metasurfaces and the conducting plane with the feeding source was then fabricated and the radiation characteristics were measured. A maximum gain of 17dBi has been measured with 8% 3dB-bandwidth showing a broadband performance. The radiation patterns extracted from the model for 13.4GHz and 14.2GHz are presented and compared with the measured ones in Fig. 7. Very small discrepancies are observed, validating the proposed concept.

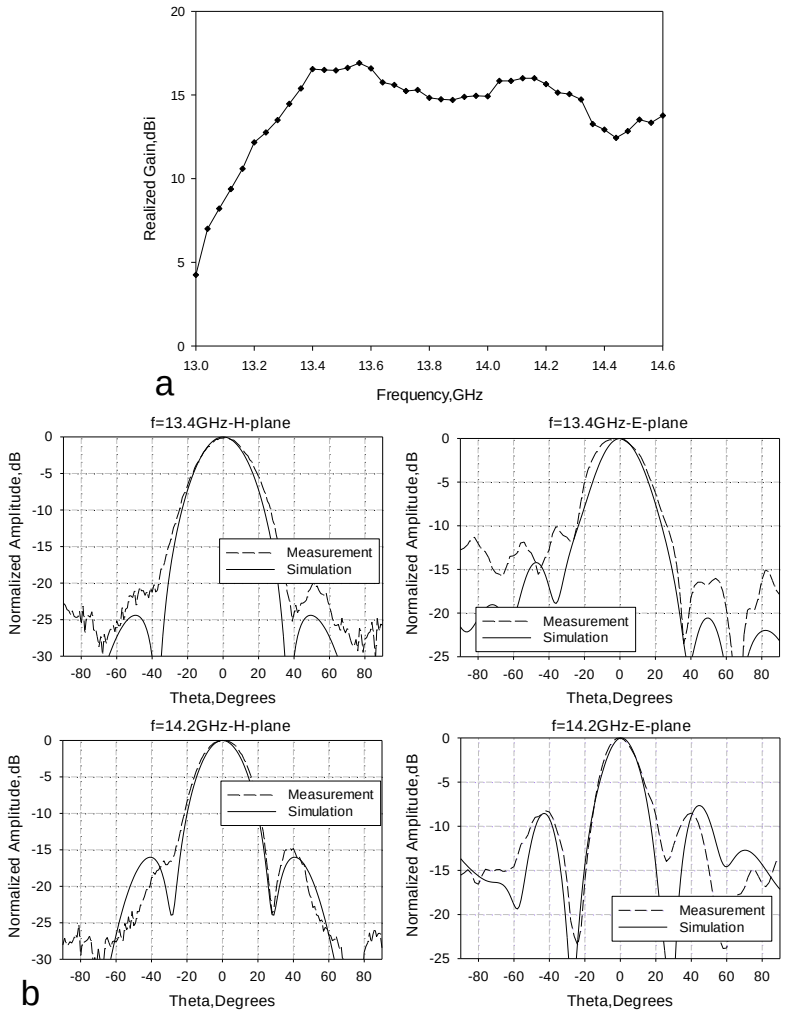

FIG. 7 (a) Measured realized gain and (b) Radiation patterns comparison between the measured and simulated results for the proposed structure. H-plane and E-plane patterns are shown at 13.4GHz and 14.2GHz.

5. Conclusion

To conclude, we have demonstrated a composite metamaterial structure with broadband NZI response. A potential application of these metasurfaces is presented, for broad frequency range directive emission in the microwave regime. We envision that this is just one of the multiple potential applications of the subwavelength broadband NZI metasurfaces, such as cloaking, super-reflection and tunnelling.

References

[1] P. Moitra, Y. Yang, Z. Anderson, I. Kravchenko, D. Briggs, and J. Valentine, Nat. Photonics 7, 791 (2013).

[2] R. Maas, J. Parsons, N. Engheta and A. Polman, Nat. Phot.. 7, 907 (2013).

[3] R. J. Pollard, A. Murphy, W. R. Hendren, P. R. Evans, R. Atkinson, G. A. Wurtz, A.V. Zayats, and V. A. Podolskiy, Phys.Rev. Lett. 102, 127405 (2009).

[4] Shuang Zhang, Wenjun Fan, N. C. Panoiu, K. J. Malloy, R. M. Osgood, and S. R. J. Brueck, Phys. Rev.Lett. 95, 137404 (2005).

[5] X. Zhang, M. Davanc¸o, Y. Urzhumov, G. Shvets, and S. R. Forrest, Phys. Rev. Lett. 101, 267401 (2008).

[6] T. Ergin, N. Stenger, P. Brenner, J. B. Pendry, and M. Wegener, Science 328, 337 (2010).

[7] E. Kallos, C. Argyropoulos, Y. Hao, and A. Alú , Phys. Rev. B 84, 045102 (2011).

[8] P. Y. Chen, C. Argyropoulos, and A. Alù, Phys. Rev. Lett. 111, 233001 (2013).

[9] J. Hao, W. Yan, and M. Qiu, Appl. Phys. Lett. 96, 101109 (2010).

[10] R. Liu, Q. Cheng, T. Hand, J. J. Mock, T. J. Cui, S. A. Cummer, and D. R. Smith, Phys. Rev. Lett. 100, 023903 (2008).

[11] M Silveirinha and N. Engheta, Phys. Rev.Lett. **97,** 157403 (2006).

[12] B. Edwards, A. Alù, M. G. Silveirinha, and N. Engheta, J. Appl. Phys. 105, 044905 (2009).

[13] D. C. Adams,S. Inampudi, T. Ribaudo, D. Slocum, S. Vangala, N. A. Kuhta, W. D. Goodhue, V. A. Podolskiy, and D. Wasserman, Phys. Rev. Lett. 107, 133901 (2011).

[14] F. Falcone, T. Lopetegi, M. A. G. Laso, J. D. Baena, J. Bonache, M. Beruete, R. Marqués, F. Martín, and M. Sorolla, Phys. Rev. Lett. 93, 197401 (2004).

[15] N.Yu and F. Capasso, Nat. Mat., 13, 139 (2014).

[16] B. Temelkuaran, M. Bayindir, E. Ozbay, R. Biswas, M. M. Sigalas, G. Tuttle, and K. M. Ho, J. Appl. Phys. 87, 603 (2000).

[17] S. Enoch, G. Tayeb, P. Sabouroux, N. Guerin, and R. Vincent, Phys. Rev. Lett. 89, 213902, (2002)

[18] E. Saenz, K. Guven, E. Ozbay, I. Ederra, and R. Gonzalo, Appl. Phys. Lett. 92, 204103 (2008).

[19] S.Wang, A. P. Feresidis, G. Goussetis and J. C. Vardaxoglou, Electr. Lett. 40, 405 (2004).

[20] L. Zhou, H. Li, Y. Qin, Z. Wei, and C. T. Chan, Appl. Phys. Lett. 86, 101101 (2005).

[21] A. Ourir, A. de Lustrac, and J.-M. Lourtioz, Appl. Phys. Lett. 88, 084103 (2006).

[22] D. Sievenpiper, L. Zhang, R. F. J. Broas, N. G. Alexopoulos, and E. Yablonovitch, IEEE Trans. Microwave Theory Tech. 47, 2059 (1999).

[23] D. R. Smith, Phys. Rev. E 81, 036605 (2010).

[24] D. R. Smith, D. C. Vier, Th. Koschny, and C. M. Soukoulis, Phys. Rev. E **71**, 036617 (2005).

[25] Z. H. Jiang, J. A. Bossard, X. Wang, and D. H. Werner, J. Appl. Phys. 109, 013515 (2011).

[26] A. Alú, Phys. Rev. B 83, 081102(R) (2011).

[27] CST Microwave studio